X-Ray Based Subpicosecond Electron Bunch Characterization Using 90° Thomson Scattering

W. P. Leemans,[1,*] R. W. Schoenlein,[1,†] P. Volfbeyn,[1,*] A. H. Chin,[2] T. E. Glover,[1,†] P. Balling,[1,†]
M. Zolotorev,[1,*] K. J. Kim,[1,*] S. Chattopadhyay,[1,*] and C. V. Shank[1,2,†]

[1]*Ernest Orlando Lawrence Berkeley National Laboratory, University of California at Berkeley, Berkeley, California 94720*
[2]*Physics Department, University of California at Berkeley, Berkeley, California 94720*
(Received 17 June 1996; revised manuscript received 23 September 1996)

X rays produced by 90° Thomson scattering of a femtosecond, near infrared, terawatt laser pulse of a 50 MeV electron beam are shown to be an effective diagnostic to measure transverse and longitudinal density distributions of an electron beam (e beam) with subpicosecond time resolution. The laser beam was focused onto the e-beam waist, generating 30 keV x rays in the forward direction. The transverse and longitudinal e-beam structures have been obtained by measuring the intensity of the x-ray beam, while scanning the laser beam across the e beam in space and time. The e-beam divergence has been obtained through measurement of spatial and spectral characteristics of the scattered x-ray beam. [S0031-9007(96)01621-3]

PACS numbers: 29.27.Fh, 13.60.Fz, 42.62.Hk

The advent of subpicosecond terawatt laser systems based on chirped pulse amplification [1] has renewed the interest in bright sources of high-energy photons that employ scattering between laser light and relativistic electrons [2,3], as well as in diagnostics and control of relativistic particle beams. Production of femtosecond x-ray pulses using such scattering requires either development of very short electron bunches [4] or a scattering geometry in which the photon and electron beams cross at 90° and are both tightly focused [3]. In this geometry the interaction time between the electron beam and laser beam is limited to the transverse rather than the longitudinal transit time of the laser pulse across the electron beam. Ultrashort x-ray pulses can then be generated from long electron bunches [5]. Another fascinating and immediate consequence of the 90° scattering geometry is the possibility to measure the phase space properties of femtosecond (fs) length electron beam slices. In this Letter we present measurements of transverse electron beam distribution and divergence of 100 fs long temporal slices, as well as longitudinal bunch shape of a 50 MeV electron beam, by analyzing x rays with energy up to 30 keV. The x rays were generated by Thomson scattering terawatt laser pulses (Compton recoil can be neglected), with a photon energy of 1.5 eV, off the electron beam.

Historically, soon after the invention of the laser, Fiocco and Thompson [6] used Thomson scattering to measure the energy distribution of an electron beam. Recently, transverse e-beam sizes as small as 70 nm were measured, by scanning a high energy electron beam across the intensity fringes of an optical standing wave [7]. With femtosecond laser pulses, longitudinally resolved measurement of e-beam phase space characteristics becomes possible. Development of this kind of technique will be increasingly important for diagnosing electron bunches in future accelerators.

Figure 1 presents a schematic of the experiment in which the 90° Thomson scattering geometry has been used. The experiments were conducted at the Beam Test Facility (BTF) [8] of the Center for Beam Physics at the Berkeley Laboratory. The linear accelerator (linac) injector of the Advanced Light Source was used in conjunction with a terawatt short pulse laser system. Electron bunches with energy of 50 MeV (energy spread 0.2%–0.4%) containing typically 1.3 nC of charge within a 10–15 ps (rms) bunch length were produced by the linac at a 2 Hz repetition rate, and transported using bend magnets and quadrupoles (BTF line) to an interaction chamber. The electron beam was focused in the interaction chamber where it scattered against the laser beam. After the interaction chamber, a 60° bend magnet deflected the electron beam onto a beam dump, away from the forward scattered x rays.

To measure the spot size (and position) of the electron beam at the interaction point (IP), a 2 μm thick Al-coated nitrocellulose foil, mounted on a retractable plunger at 45° with respect to the beam, was installed in the chamber. An image of the electron beam was obtained from optical transition radiation (OTR) [9]. The image was relayed onto a 16 bit charge-coupled device (CCD) camera or optical streak camera using a small f-number telescope. The spatial resolution of the imaging system was 14 μm.

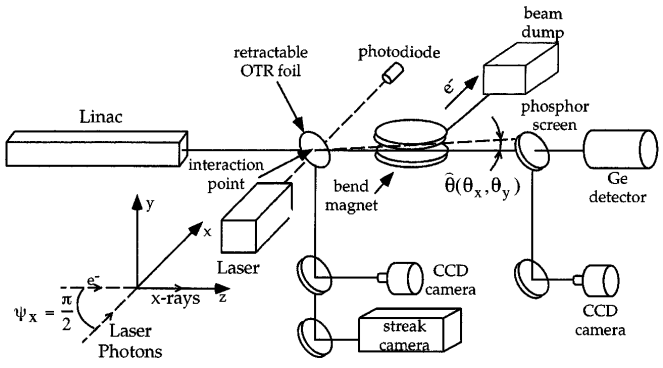

FIG. 1. Schematic of the experimental setup.

 0031-9007/96/77(20)/4182(4)$10.00

Electron beam spot sizes as small as 35 μm have been measured.

The femtosecond laser system, with center wavelength at 800 nm, is based on chirped pulse amplification in Ti:Al_2O_3 [1,10]. The Kerr lens mode-locked oscillator operates at the fourth subharmonic of the 500 MHz master oscillator source for the linac. Individual laser oscillator pulses are extracted at a 10 Hz repetition rate, and are temporally stretched using a grating and a telescope based on a parabolic reflector. Amplification to the 100–200 mJ range is achieved in an 8-pass preamplifier and a 3-pass power amplifier pumped by a Q-switched Nd:YAG laser. The amplified pulses are temporally compressed in a vacuum chamber using a grating pair and are propagated to the e-beam/laser interaction chamber through an evacuated beam line. Amplified laser pulses as short as 50 fs (2 TW peak power) have been produced but typical operating parameters for the experiment are 100 fs long pulses containing about 40 mJ energy. A 75 cm radius of curvature mirror is used to focus the S-polarized amplified laser pulses to about a 30 μmm diameter spot at the IP (measured by a CCD camera at an equivalent image plane outside the vacuum chamber).

Synchronization between the laser oscillator and linac is accomplished by using a phase-locked loop which dynamically adjusts the oscillator cavity length. The phase error signal is generated by mixing the fourth harmonic of the oscillator repetition frequency (generated from a photodiode) with the master oscillator source for the linac. Timing jitter measurements (using a streak camera with time resolution of 1.5–2 ps) which simultaneously detected a laser pulse and OTR from the electron bunch indicated an rms jitter of 1–2 ps.

To monitor the arrival time of the electron bunch and laser pulse at the IP, a button-type radio-frequency pickup and a 6 ps rise time photoconductive switch were used to provide a signal from the electron beam and laser pulse, respectively. The signals were measured on a transient digitizer with 4.5 GHz bandwidth. An optical delay line was used to change the arrival time of the laser pulse. Initial spatial alignment of the beams was accomplished by optimizing the e beam and laser transmission through a cube with two 250 μm diameter intersecting orthogonal holes.

Total flux and profile of the x-ray beam were measured using a phosphor screen, located 80 cm from the IP. This phosphor has a linear energy conversion efficiency in the 10–50 keV range [11]. Visible photons from the screen are imaged onto a two dimensional (512 $\times$ 512), 16 bit CCD camera. The sensitivity of the x-ray detection system was calibrated using a I^{129} radioactive source. For a horizontal and vertical CCD binning factor of 32, the sensitivity (x rays/CCD count) of the system was measured to be 1.2 $\times$ 0.4 x-ray photons/count, and was found to be linear over at least 2 orders of magnitude. The detection system had a full collection angle of 25 mrad. The total flux within the collection angle was typically 5 $\times$ 10^4 photons.

To measure the transverse electron beam distribution for a given slice of the electron beam, we scanned the laser beam transversely across the electron beam and monitored the x-ray yield on the phosphor screen. The laser beam position was changed vertically at the interaction point, in steps of 10 μm, by changing the tilt of the focusing mirror. The plot of x ray yield vs laser position is shown in Fig. 2, together with a measurement of the time integrated, transverse e-beam size using the OTR image on the CCD camera. From the data we find that, both techniques are in good agreement and give a half-width half maximum (HWHM) vertical size of 66 μm. However, whereas the beam core overlaps, the tails are different and both non-Gaussian. This result was reproducible and may indicate real differences in the time structure of the tails of the spatial distribution of the actual beams that were being sampled, which will be discussed below. From the OTR data we also obtained an HWHM horizontal size of 47 μm.

Measurement of the electron beam divergence for a fixed longitudinal location (i.e., fixed delay time between the laser and electron beams) was done by monitoring the spatial x-ray beam profile on the phosphor screen using the CCD camera. A typical false-color picture of the radiation from the phosphor screen, produced x rays from a 300 fs electron beam slice, is shown in Fig. 3(a), and horizontal and vertical line profiles are shown in Fig. 3(b). Background radiation from electron bremsstrahlung has been subtracted. The ellipticity of the image results from astigmatism in the electron beam focusing, which, for the smaller horizontal than vertical spot size from Fig. 2, causes a stronger electron beam divergence in the horizontal (and therefore stronger x-ray beam divergence) than in the vertical direction.

To analyze the experimentally measured spatial and spectral characteristics of the x-ray beam, we have convolved the single electron Thomson scattering cross section with a Gaussian spatial and spectral distribution of photons and electrons. For our parameters, any nonlinear

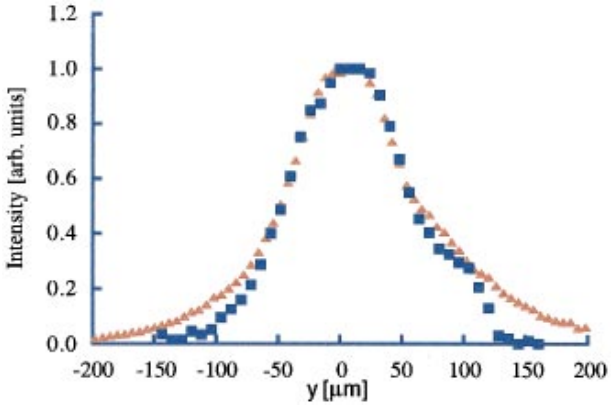

FIG. 2(color). ▲ (Triangle)—vertical line profile through an OTR image of the electron beam; ■ (square)—x-ray yield vs vertical laser beam position.

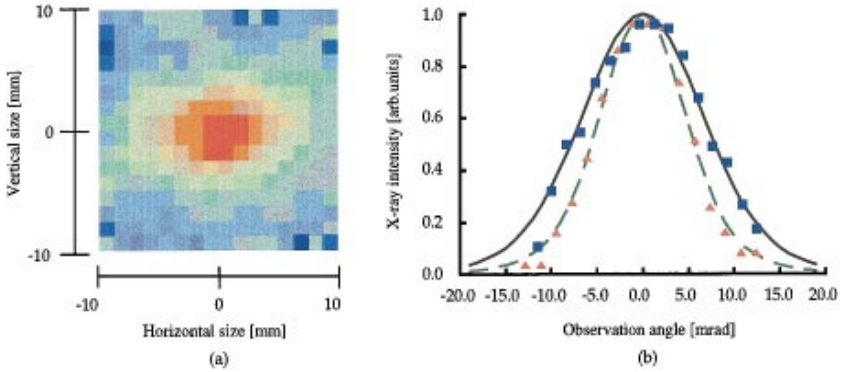

FIG. 3(color). (a) False color CCD image of the spatial profile of a 30 keV x-ray pulse on the phosphor screen, which is located 80 cm from the IP; (b) ■ (square)—horizontal line profile and fitting curve (solid line), ▲ (triangle)—vertical line profile and fitting curve (dashed line) from (a). The scale has been converted into angular units.

dependence of the electron motion on the field of the laser can be neglected as well as any recoil effects of the electron. The energy of the scattered x-ray photon U_x, for an incident single photon with frequency ω_0, is given by (for $\gamma \gg 1$) [2,3]

$$U_x = \frac{2\gamma^2\hbar\omega_0}{1 + \gamma^2\chi^2}(1 - \cos\psi). \tag{1}$$

Here ψ is the interaction angle between the electron and laser beam ($\psi = \pi/2$ in our experiments) and $\chi \ll 1$ is the scattering angle.

The scattered x-ray energy flux can be obtained by accounting for the spatial and temporal profiles of the electron and laser beams as well as by convolving the single electron spectrum [3], with the angular distribution function of the electron beam, and integrating over all energies and azimuthal angles.

For a Gaussian angular electron beam distribution and a linear polarized incident laser beam, in the x direction (see Fig. 1), we obtain, at the horizontal (vertical) observation angles θ_x (θ_y)

$$\frac{dP}{d\theta_x d\theta_y} \propto \int_0^{2\pi} d\phi \int_0^1 d\kappa F(\kappa)\kappa[1 - 4\kappa(1 - \kappa)\cos^2\phi]\exp\left[-\frac{(\theta_x - \gamma^{-1}\sqrt{\frac{1}{\kappa} - 1}\sin\phi)^2}{2\sigma_{\theta x}^2}\right] \times \exp\left[-\frac{(\theta_y + \gamma^{-1}\sqrt{\frac{1}{\kappa} - 1}\cos\phi)^2}{2\sigma_{\theta y}^2}\right]. \tag{2}$$

Here $\sigma_{\theta x}$ and $\sigma_{\theta y}$ are the rms widths of the angular distribution of the electron beam in the horizontal and vertical directions, respectively, and $F(\kappa)$ is an x-ray energy dependent function which takes into account overall detector sensitivity. We also defined $\kappa = U/U_{\max} = (1 + \gamma^2\chi^2)^{-1}$ from Eq. (1), where $U_{\max} = 2\gamma^2\hbar\omega_0$ and assumed a single incident laser frequency.

By fitting the data [see Fig. 3(b)] using Eq. (2), we obtain an electron beam divergence of $\sigma_{\theta x}$ ($\sigma_{\theta y}$) = 6.3 ± 0.2 (3.9 ± 0.2) mrad. The difference between $\sigma_{\theta x}$ and $\sigma_{\theta y}$ is due to a combination of the electron beam being focused astigmatically at the IP, resulting in a tilted phase space ellipse (y, y'), and a laser spot size much smaller than the vertical electron beam size. As the laser beam crosses the focal volume of the electron beam, the complete horizontal (direction of propagation of the laser) phase space (x, x') is sampled by the laser beam. However, only electrons occupying the region in the vertical phase space defined by the spatial overlap with the laser beam will contribute to the x-ray flux. As opposed to the transition radiation based detector, the laser beam therefore acts as an optical microprobe of a finite region of the transverse phase space.

An independent estimate of the electron beam divergence was obtained by analyzing x-ray spectra measured at angles $\theta = 0$, 5, and 10 mrad [5]. For an electron beam focused to an rms spot size of 70 μm at the IP, these spectra indicated an effective angular divergence of the electron beam of 3.5–4 mrad.

The spot size measurements and beam divergence measurements imply a horizontal geometric slice emittance $\sigma_x\sigma_{\theta x}$ for the electron beam of 0.25 ± 0.03 mm mrad. A linac beam emittance of 0.32 ± 0.02 mm mrad was measured using a time-integrated quadrupole scan technique [12], and was found to be in reasonable agreement with the x-ray slice measurements.

To measure the longitudinal electron beam distribution at the IP, the x-ray flux on the phosphor screen was monitored as a function of the delay between the laser and e beams (changed in 1 ps time steps). An example of a 60 ps long scan is shown in Fig. 4(a), where background radiation has again been subtracted. The scans typically showed a 5 ps wide peak sitting on a 20 ps wide pedestal. The amplitude of the narrow peak was typically 2 to 3 times larger than the pedestal. The detail seen in the longitudinal distribution is in contrast to the time resolved

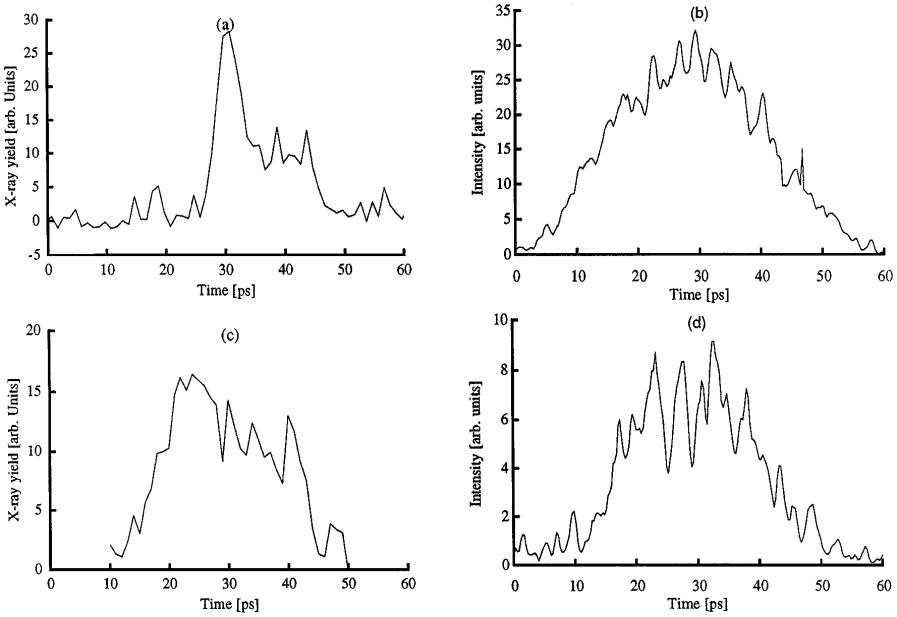

FIG. 4. X-ray yield vs delay time between the laser and electron beams for a lattice with (a) large and (c) small chromatic aberrations; time resolved OTR image from a streak camera for a magnetic lattice with (b) large and (d) small chromatic aberrations.

OTR from the streak camera which typically showed a 25–30 ps wide electron beam without any sharp time structure [Fig. 4(b)]. Also, the Thomson diagnostic was found to be much more sensitive to linac and lattice changes, as opposed to the streak camera measurements.

Magnetic lattice calculations indicate that the difference could be caused by chromatic aberrations of the lattice: for an electron bunch which exhibits a finite time-correlated energy spread (chirp), each time slice will be focused at a different longitudinal location. In the calculations, an energy change of 0.25% increases the vertical spot size by a factor of 2 at the IP, compared to best focus, resulting in a proportional reduction in vertical overlap between the laser and electron beams, and hence in x-ray yield.

To experimentally test this hypothesis, we implemented a magnetic lattice with about a 5 times smaller chromatic aberration at the IP. As shown in Fig. 4(c), now the temporal scan is in much better agreement with the time-resolved OTR [Fig. 4(d)]. In addition, nonisochronicity of this lattice also resulted in a slightly shorter bunch.

In summary, we have presented first experimental results of an electron beam diagnostic based on x-ray measurements from 90° Thomson scattering of 100 fs long laser pulses. The total flux of x rays was on the order of 5×10^4 for typical laser and electron beam parameters in the experiment. From a study of x-ray beam images and total flux, we have obtained the transverse electron beam phase space distribution of essentially a 300 fs slice of the electron beam. By scanning the laser beam in time along the electron bunch, we have measured not only the longitudinal density distribution, but also found that the Thomson scattering technique can become a powerful tool to measure longitudinal phase space properties.

One of us (W. P. L.) thanks E. Esarey for useful conversations. We also thank L. Archambault, A. Belkacem, T. Byrne, M. Conde, M. de Loos, J. Dougherty, M. Faiguenblatt, A. Ghiorso, R. Govil, A. Jackson, D. Massoletti, B. van der Geer, and A. Zholents for their contributions. This work is supported by the Department of Energy under Contracts No. AC03-76SF00098 and No. FDDEFG-03-95ER-40936 and by the National Science Foundation under Grant No. PHY-9512693.

*Center for Beam Physics, Accelerator and Fusion Research Division.
†Material Sciences Division.

[1] D. Strickland and G. Mourou, Opt. Commun. **56**, 219 (1985).
[2] P. Sprangle *et al.*, J. Appl. Phys. **72**, 5032 (1992).
[3] K. J. Kim, S. Chattopadhyay, and C. V. Shank, Nucl. Instrum. Methods Phys. Res., Sect. A **341**, 351 (1994).
[4] P. Kung *et al.*, Phys. Rev. Lett. **73**, 967 (1994); M. Uesaka *et al.*, Phys. Rev. E **50**, 3068 (1994).
[5] R. W. Schoenlein *et al.*, Science **274**, 236 (1996).
[6] G. Fiocco and E. Thompson, Phys. Rev. Lett. **10**, 89 (1963); R. H. Milburn, Phys. Rev. Lett. **10**, 75 (1963).
[7] T. Shintake, Nucl. Instrum. Methods Phys. Res., Sect. A **311**, 453 (1992).
[8] W. P. Leemans *et al.*, in *Proceedings of the 15th Particle Accelerator Conference, 1993* (IEEE, Piscataway, NJ, 1993), p. 83.
[9] L. Wartski *et al.*, J. Appl. Phys. **46**, 3644 (1975).
[10] C. LeBlanc *et al.*, Opt. Lett. **18**, 140 (1993).
[11] D. P. Trauernecht and R. Van Metter, Proc. SPIE Int. Soc. Opt. Eng. **914**, 100 (1988).
[12] J. Bengtson, W. Leemans, and T. Byrne, in *Proceedings of the 15th Particle Accelerator Conference, 1993* (Ref. [8]), p. 567.